Electronic Supplementary Material (ESI) for Physical Chemistry Chemical Physics.

Exploration of hydrogen bond networks and potential energy surfaces of methanol clusters with a two-stage clustering algorithm

Po-Jen Hsu,[†‡] Kun-Lin Ho,[†] Sheng-Hsien Lin,[‡†] and Jer-Lai Kuo[†]

† Institute of Atomic and Molecular Sciences, Academia Sinica, Taipei, Taiwan

‡ Department of Applied Chemistry, National Chiao Tung University, Hsinchu, Taiwan

Contents:

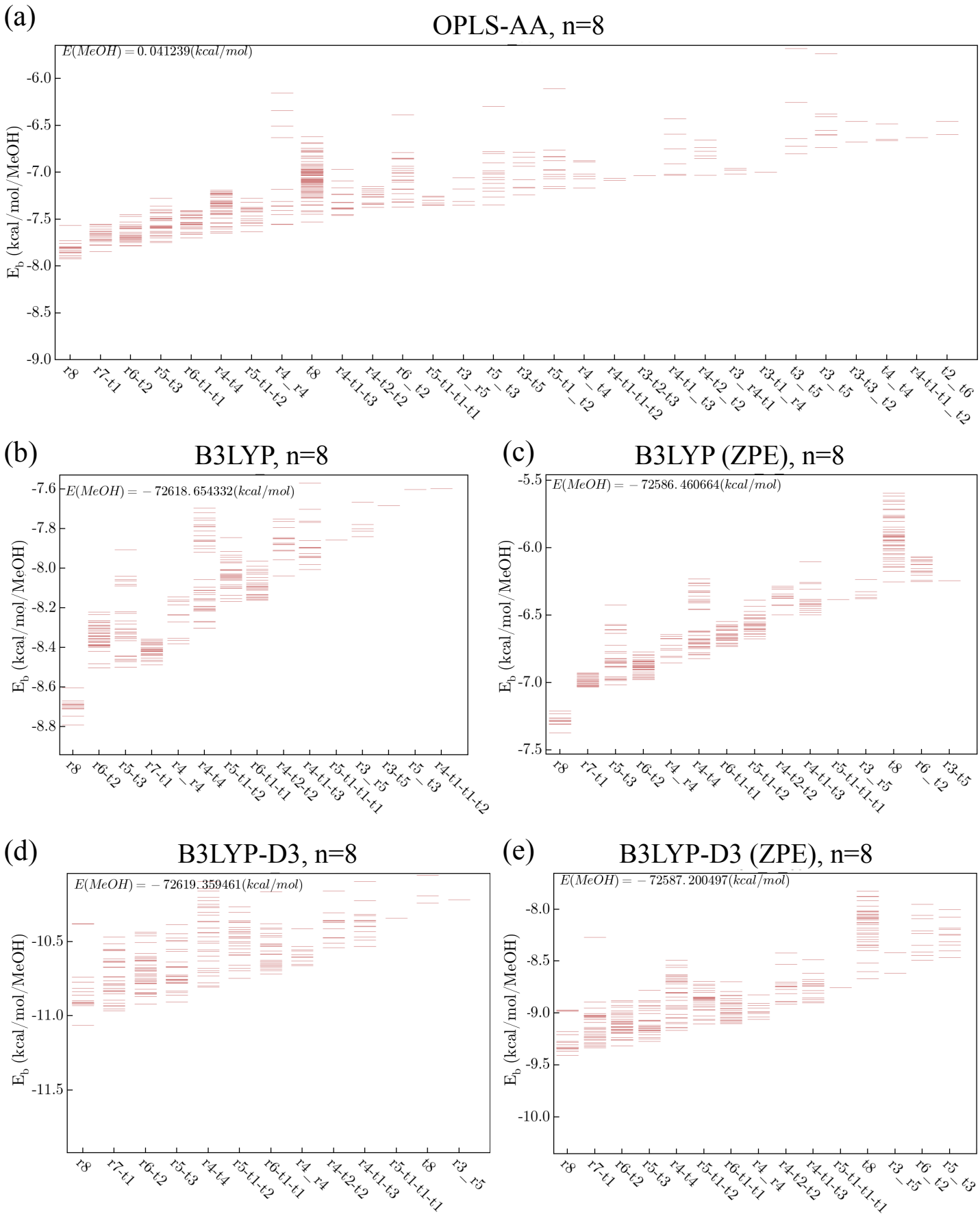

Figure 1s: Binding energy (kcal/mol/MeOH) of $(MeOH)_8$ versus topology labels under (a) OPLS-AA, (b) B3LYP, (c) B3LYP with zero-point energy correction, (d) B3LYP-D3, and (c) B3LYP-D3 with zero-point energy correction.

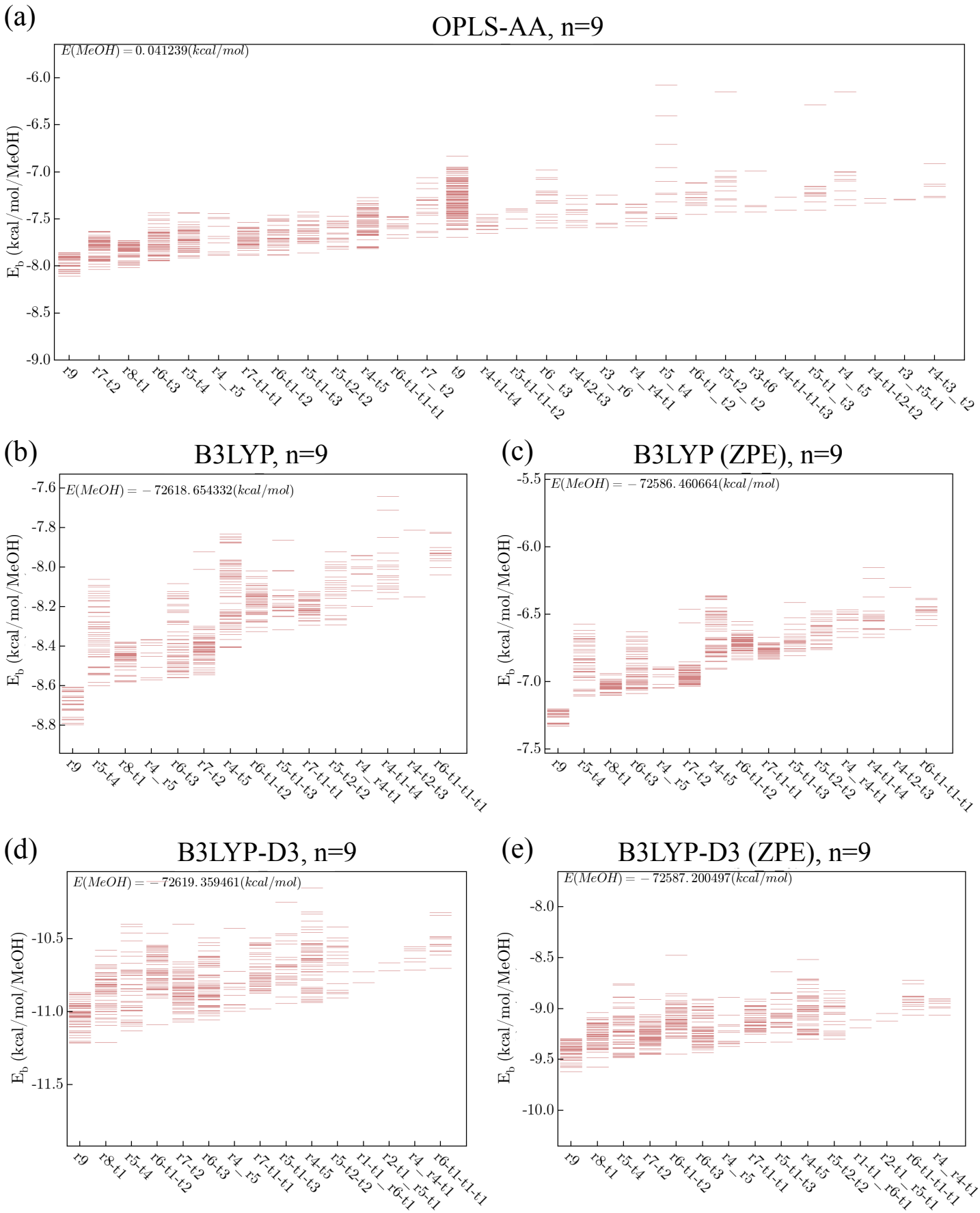

Figure 2s: Binding energy (kcal/mol/MeOH) of $(MeOH)_9$ versus topology labels under (a) OPLS-AA, (b) B3LYP, (c) B3LYP with zero-point energy correction, (d) B3LYP-D3, and (c) B3LYP-D3 with zero-point energy correction.

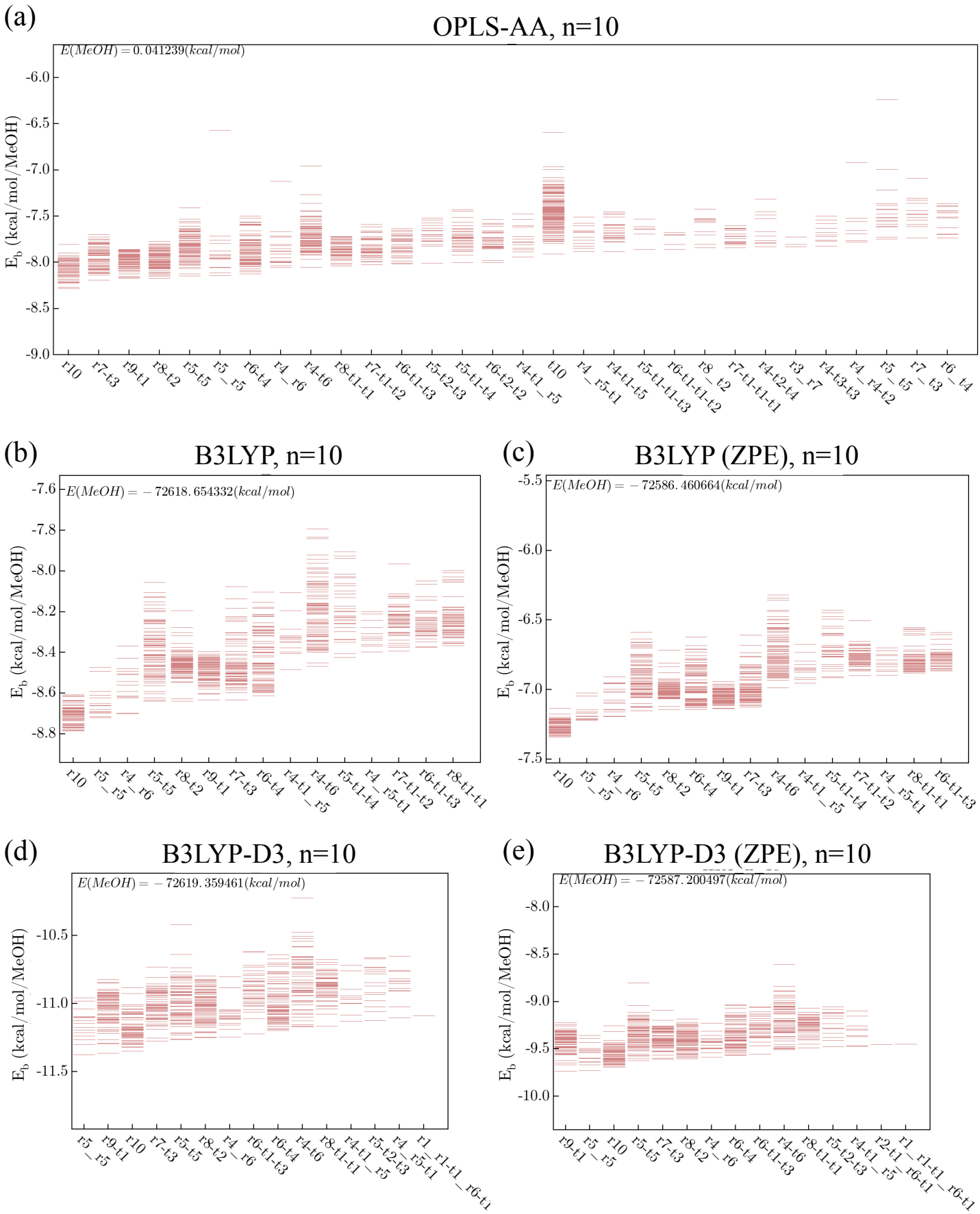

Figure 3s: Binding energy (kcal/mol/MeOH) of $(MeOH)_{10}$ versus topology labels under (a) OPLS-AA, (b) B3LYP, (c) B3LYP with zero-point energy correction, (d) B3LYP-D3, and (c) B3LYP-D3 with zero-point energy correction.

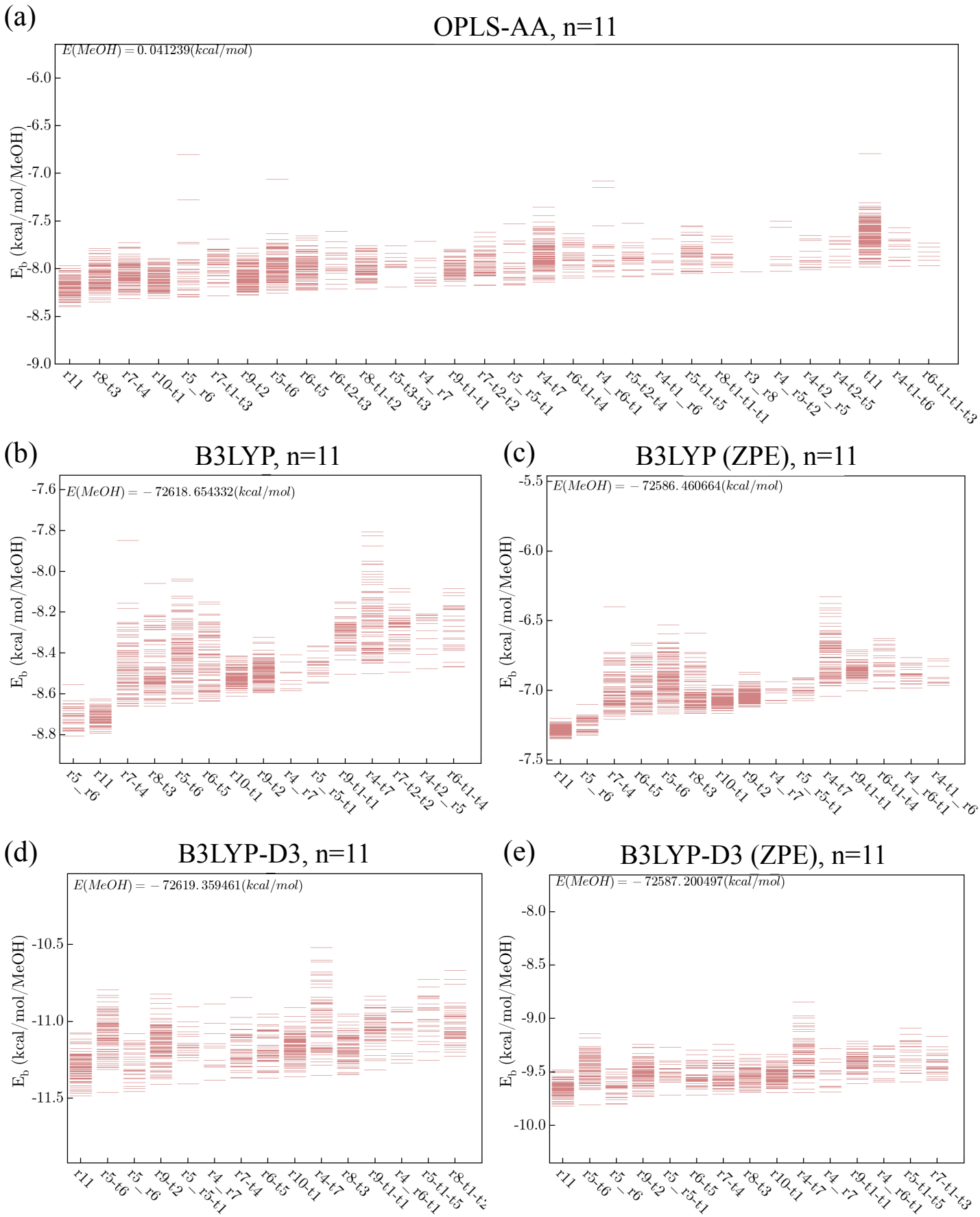

Figure 4s: Binding energy (kcal/mol/MeOH) of $(MeOH)_{11}$ versus topology labels under (a) OPLS-AA, (b) B3LYP, (c) B3LYP with zero-point energy correction, (d) B3LYP-D3, and (c) B3LYP-D3 with zero-point energy correction.

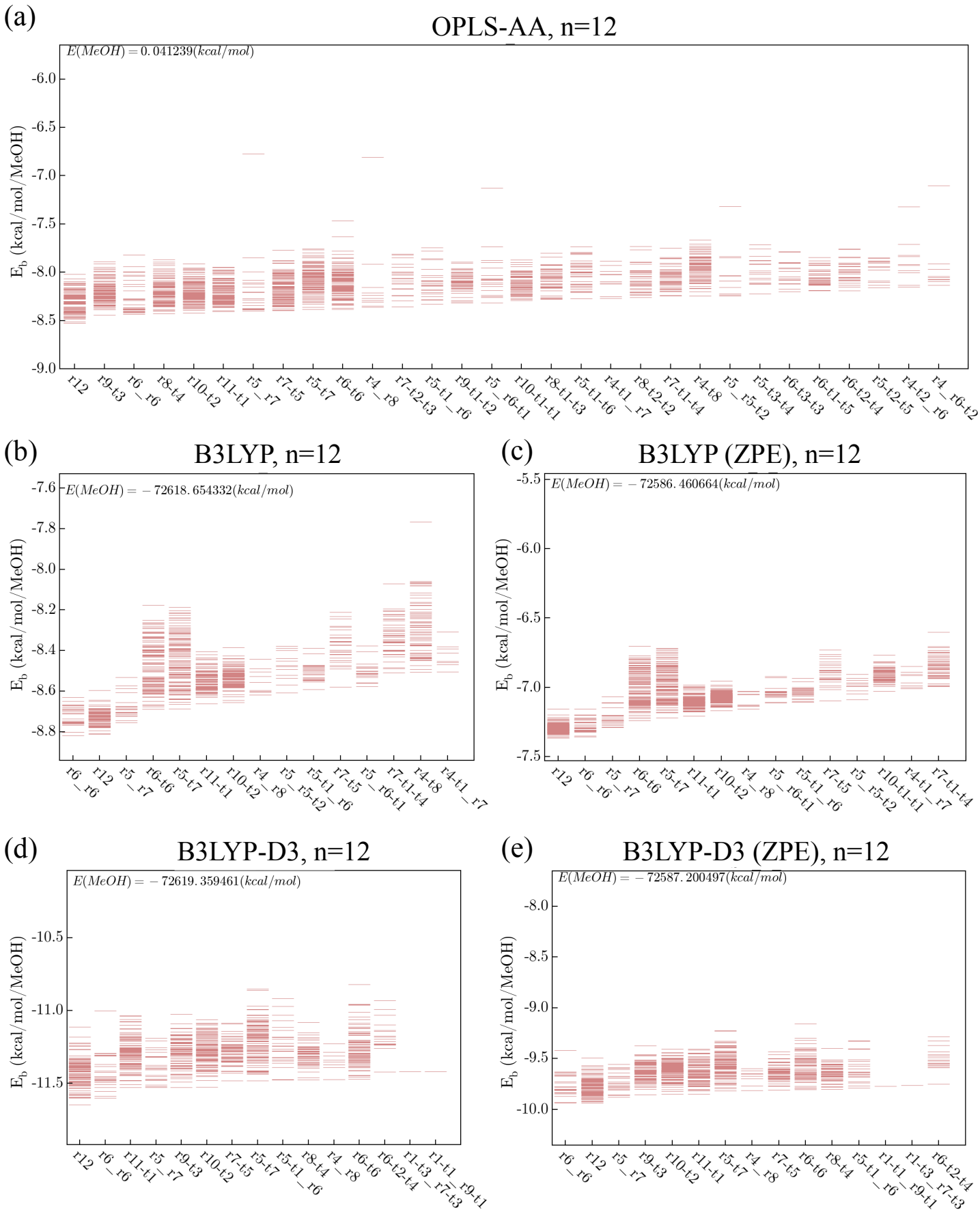

Figure 5s: Binding energy (kcal/mol/MeOH) of $(MeOH)_{12}$ versus topology labels under (a) OPLS-AA, (b) B3LYP, (c) B3LYP with zero-point energy correction, (d) B3LYP-D3, and (c) B3LYP-D3 with zero-point energy correction.

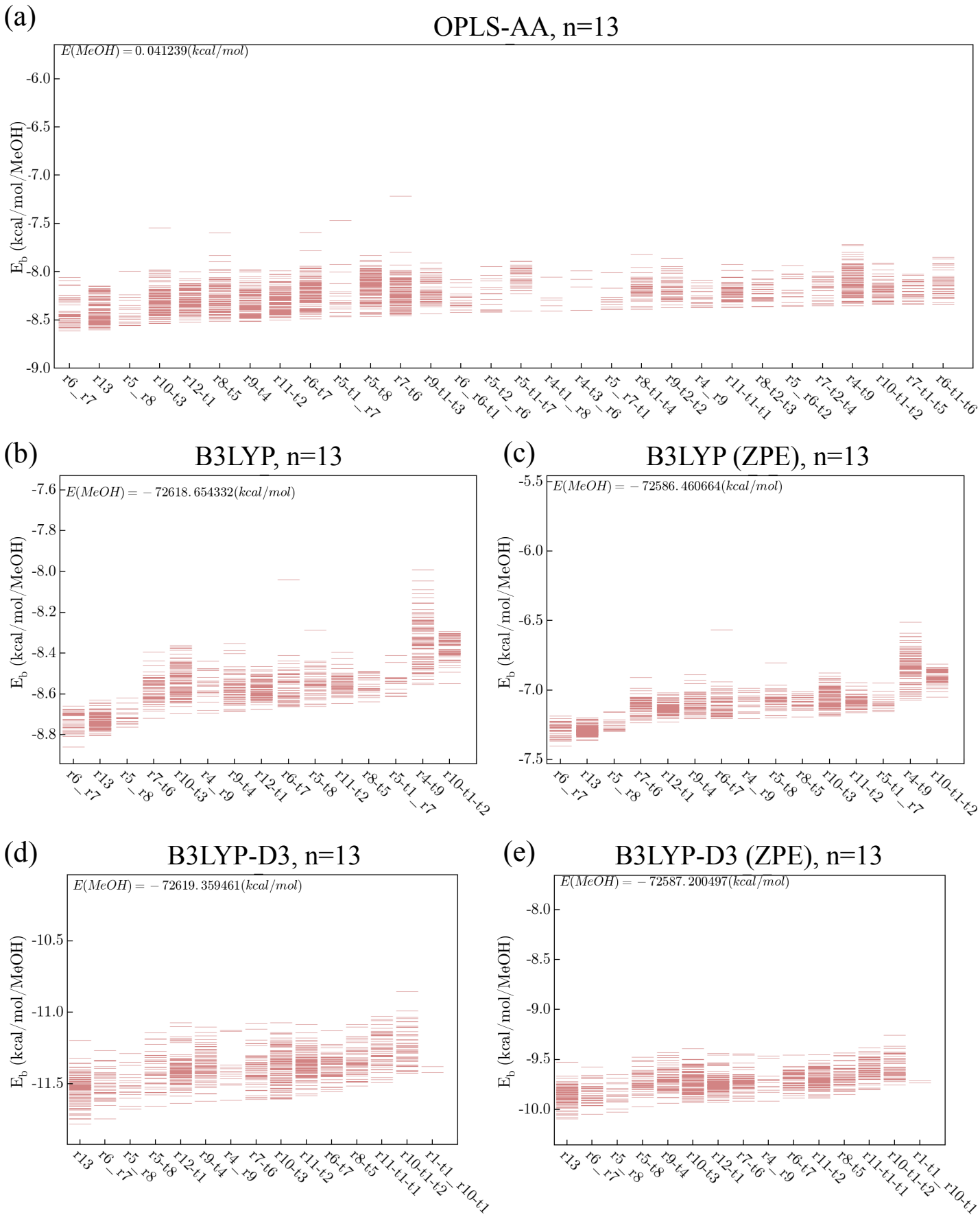

Figure 6s: Binding energy (kcal/mol/MeOH) of $(MeOH)_{13}$ versus topology labels under (a) OPLS-AA, (b) B3LYP, (c) B3LYP with zero-point energy correction, (d) B3LYP-D3, and (c) B3LYP-D3 with zero-point energy correction.

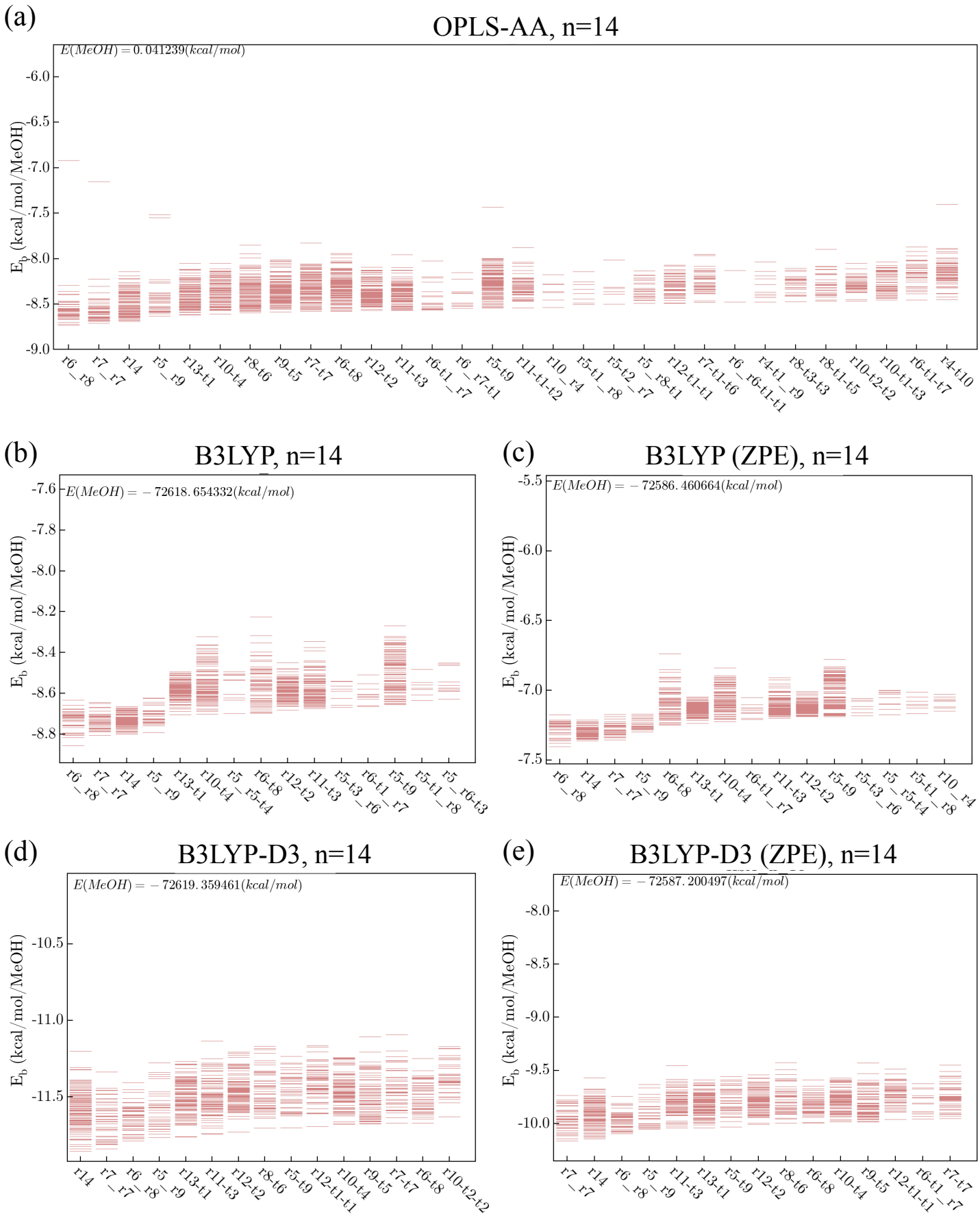

Figure 7s: Binding energy (kcal/mol/MeOH) of $(MeOH)_{14}$ versus topology labels under (a) OPLS-AA, (b) B3LYP, (c) B3LYP with zero-point energy correction, (d) B3LYP-D3, and (c) B3LYP-D3 with zero-point energy correction.

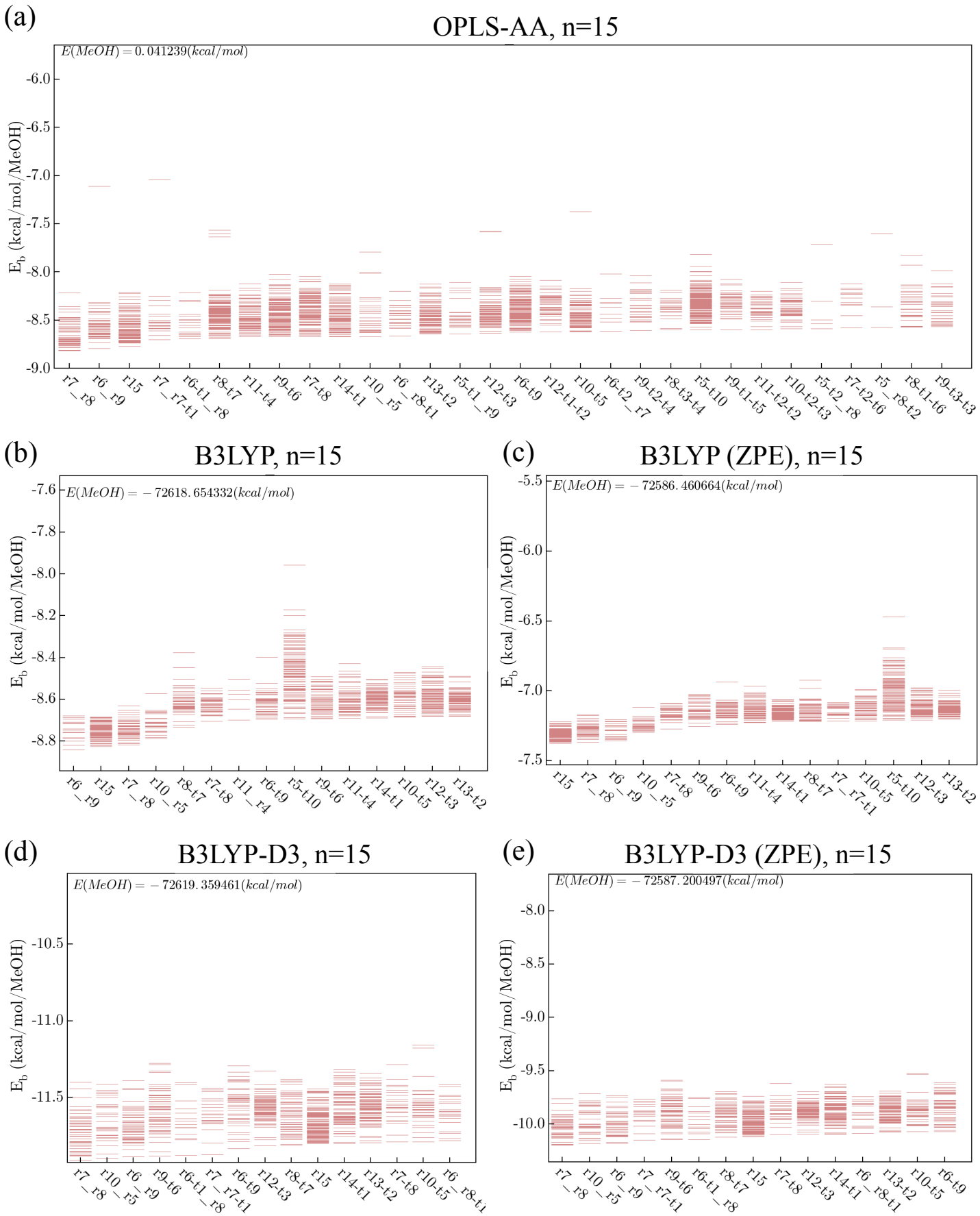

Figure 8s: Binding energy (kcal/mol/MeOH) of $(MeOH)_{15}$ versus topology labels under (a) OPLS-AA, (b) B3LYP, (c) B3LYP with zero-point energy correction, (d) B3LYP-D3, and (c) B3LYP-D3 with zero-point energy correction.

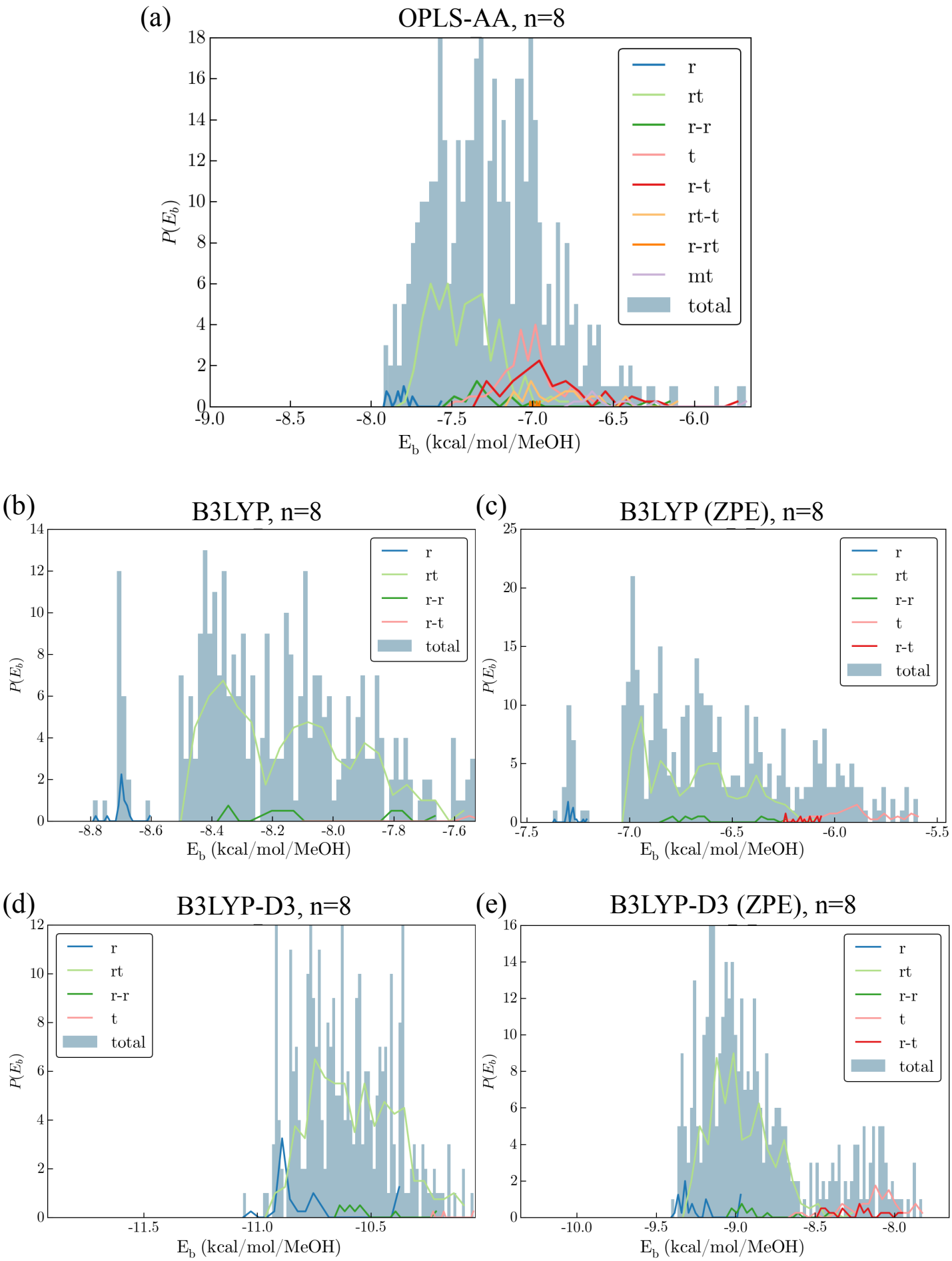

Figure 9s: Energy histograms of $(MeOH)_8$ isomers under (a) OPLS-AA, (b) B3LYP, (c) B3LYP with zero-point correction, (d) B3LYP-D3, and (e) B3LYP-D3 with zero-point correction.

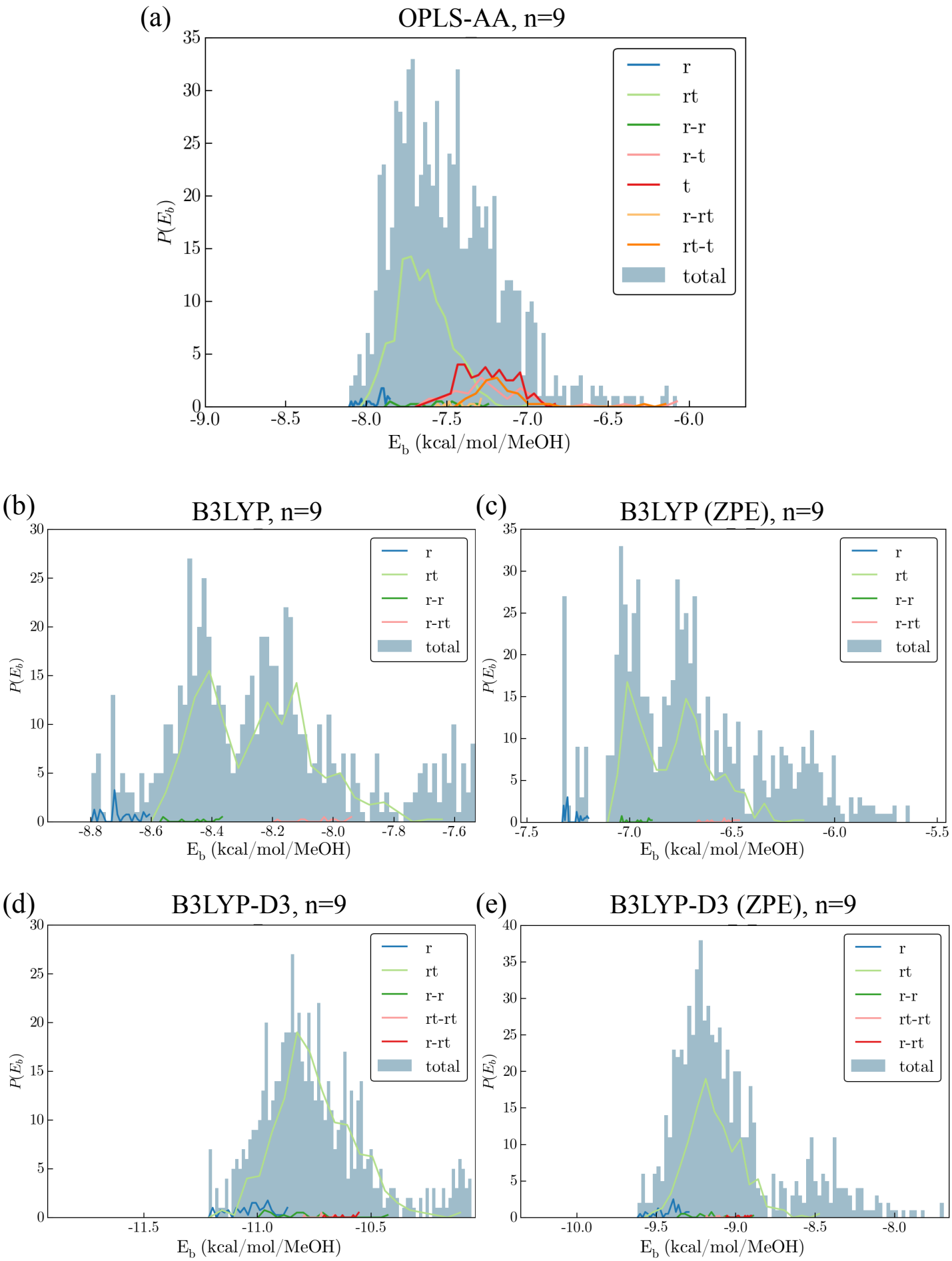

Figure 10s: Energy histograms of $(MeOH)_9$ isomers under (a) OPLS-AA, (b) B3LYP, (c) B3LYP with zero-point correction, (d) B3LYP-D3, and (e) B3LYP-D3 with zero-point correction.

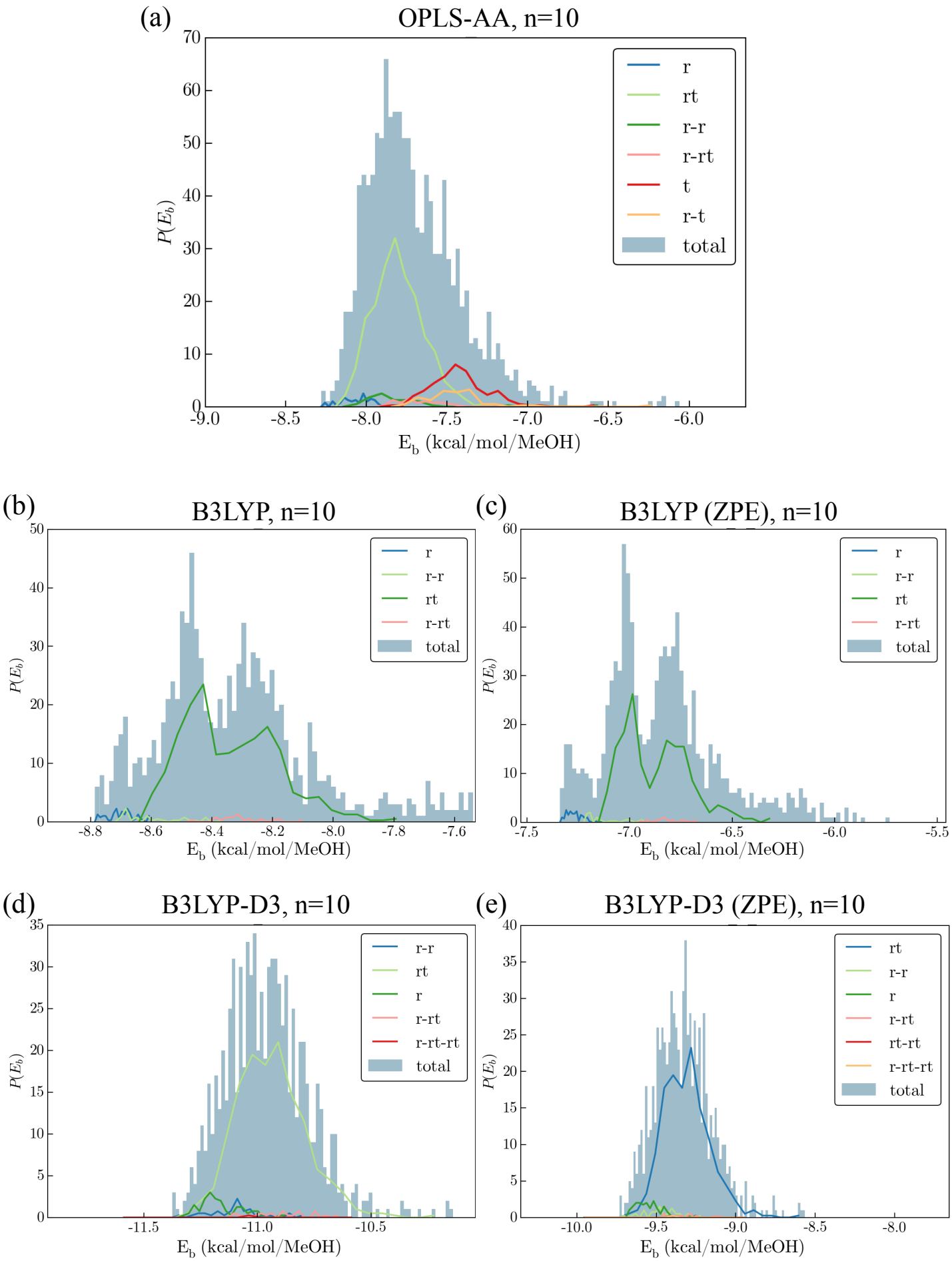

Figure 11s: Energy histograms of $(MeOH)_{10}$ isomers under (a) OPLS-AA, (b) B3LYP, (c) B3LYP with zero-point correction, (d) B3LYP-D3, and (e) B3LYP-D3 with zero-point correction.

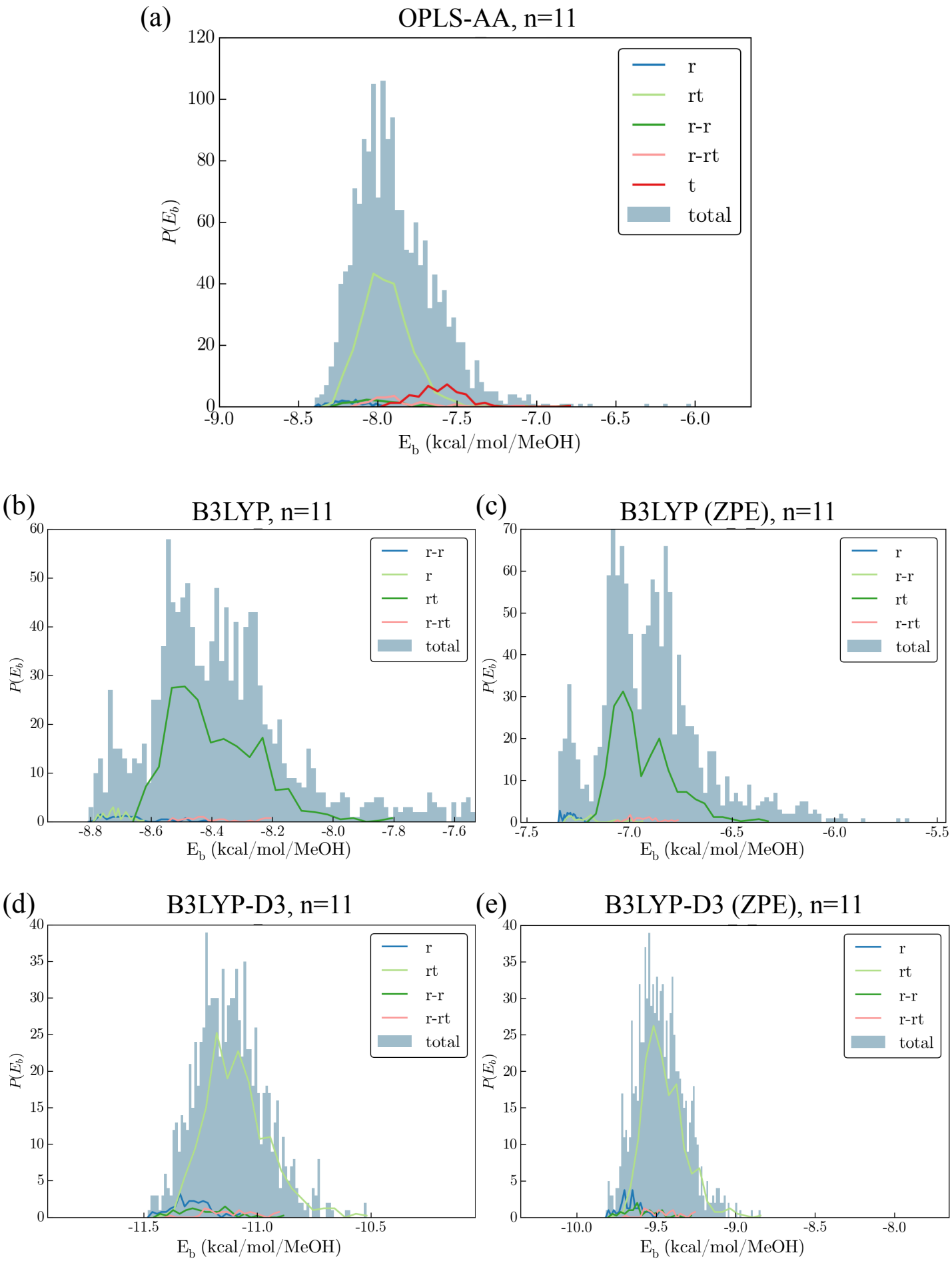

Figure 12s: Energy histograms of $(MeOH)_{11}$ isomers under (a) OPLS-AA, (b) B3LYP, (c) B3LYP with zero-point correction, (d) B3LYP-D3, and (e) B3LYP-D3 with zero-point correction.

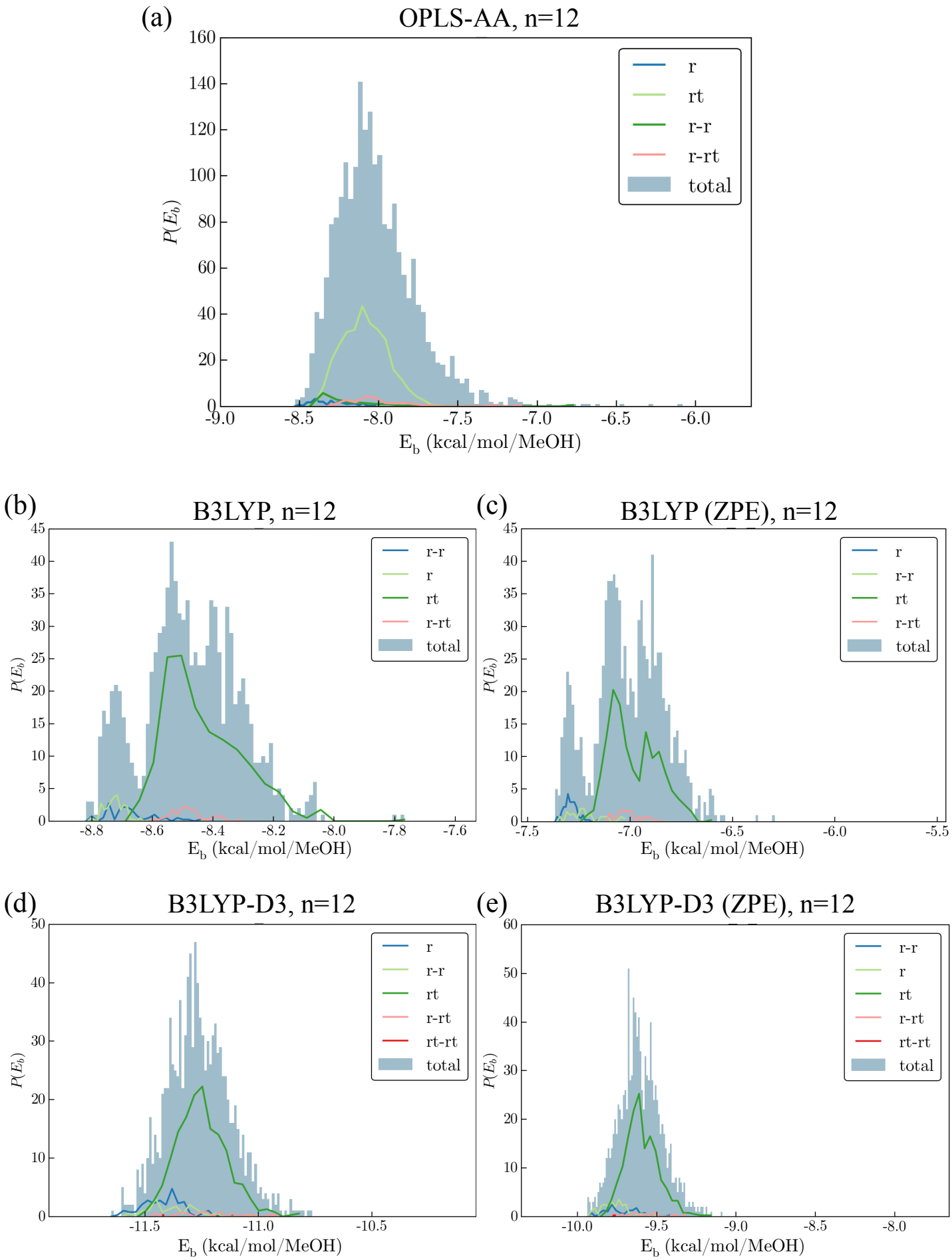

Figure 13s: Energy histograms of $(MeOH)_{12}$ isomers under (a) OPLS-AA, (b) B3LYP, (c) B3LYP with zero-point correction, (d) B3LYP-D3, and (e) B3LYP-D3 with zero-point correction.

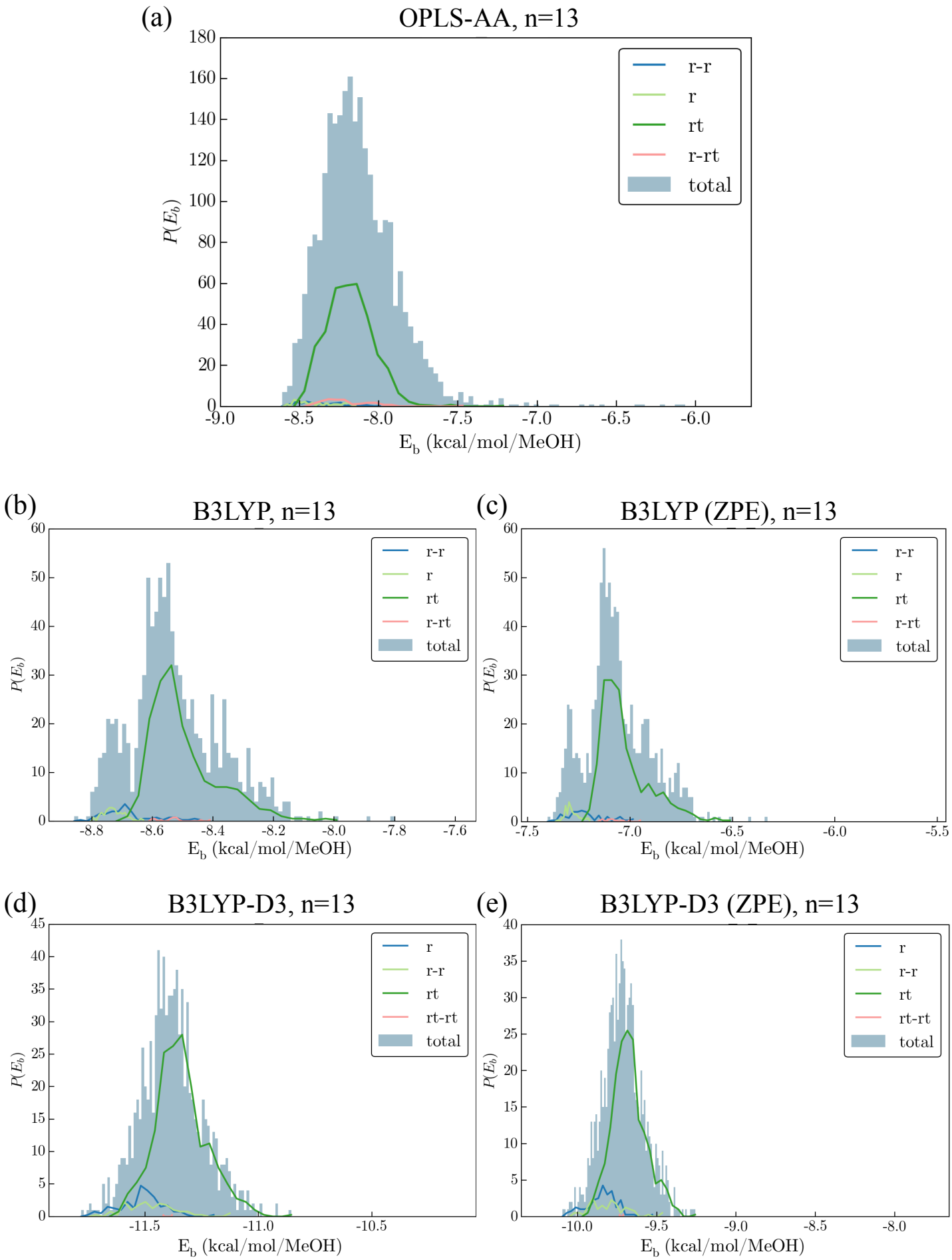

Figure 14s: Energy histograms of $(MeOH)_{13}$ isomers under (a) OPLS-AA, (b) B3LYP, (c) B3LYP with zero-point correction, (d) B3LYP-D3, and (e) B3LYP-D3 with zero-point correction.

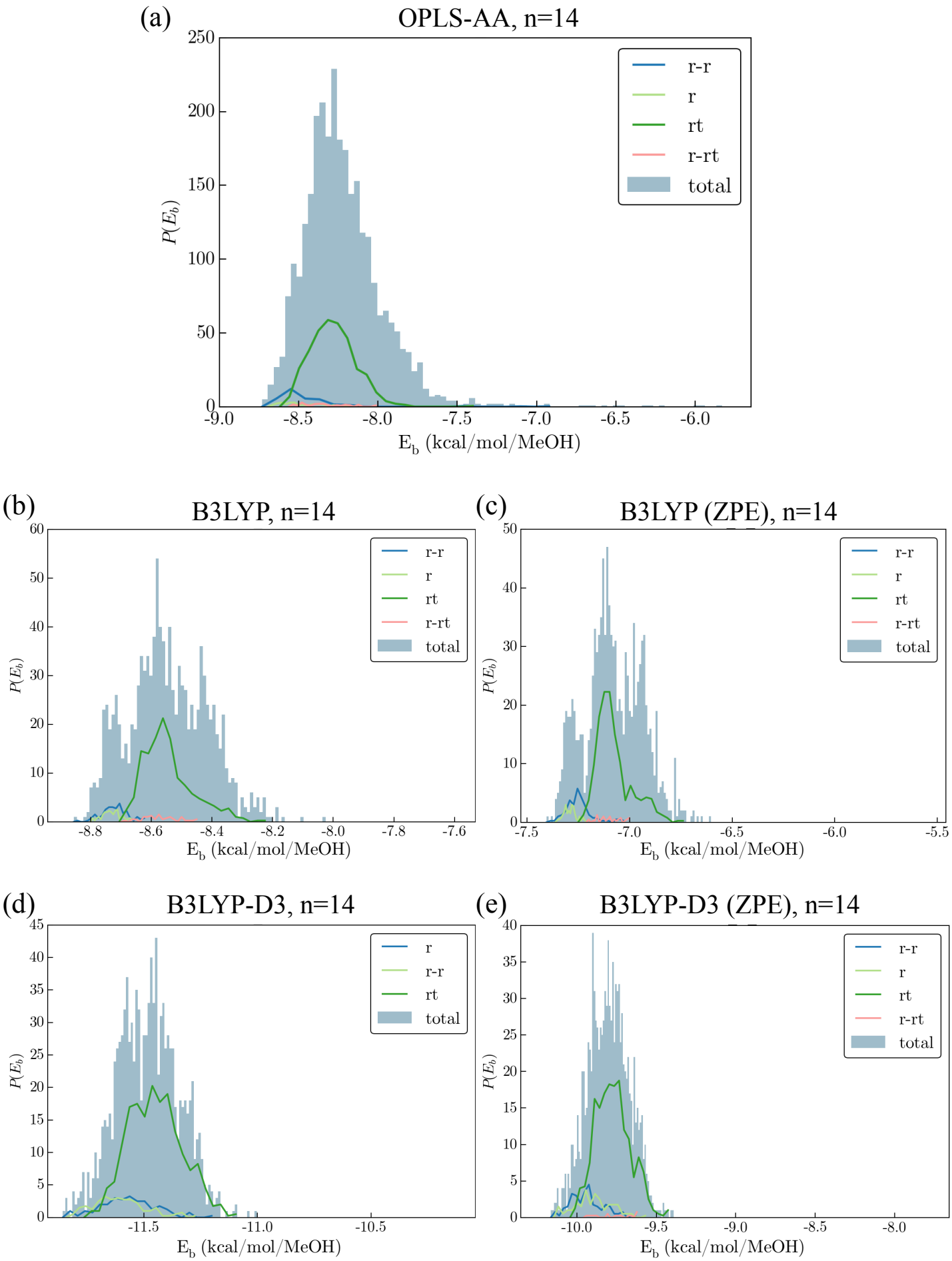

Figure 15s: Energy histograms of $(MeOH)_{14}$ isomers under (a) OPLS-AA, (b) B3LYP, (c) B3LYP with zero-point correction, (d) B3LYP-D3, and (e) B3LYP-D3 with zero-point correction.

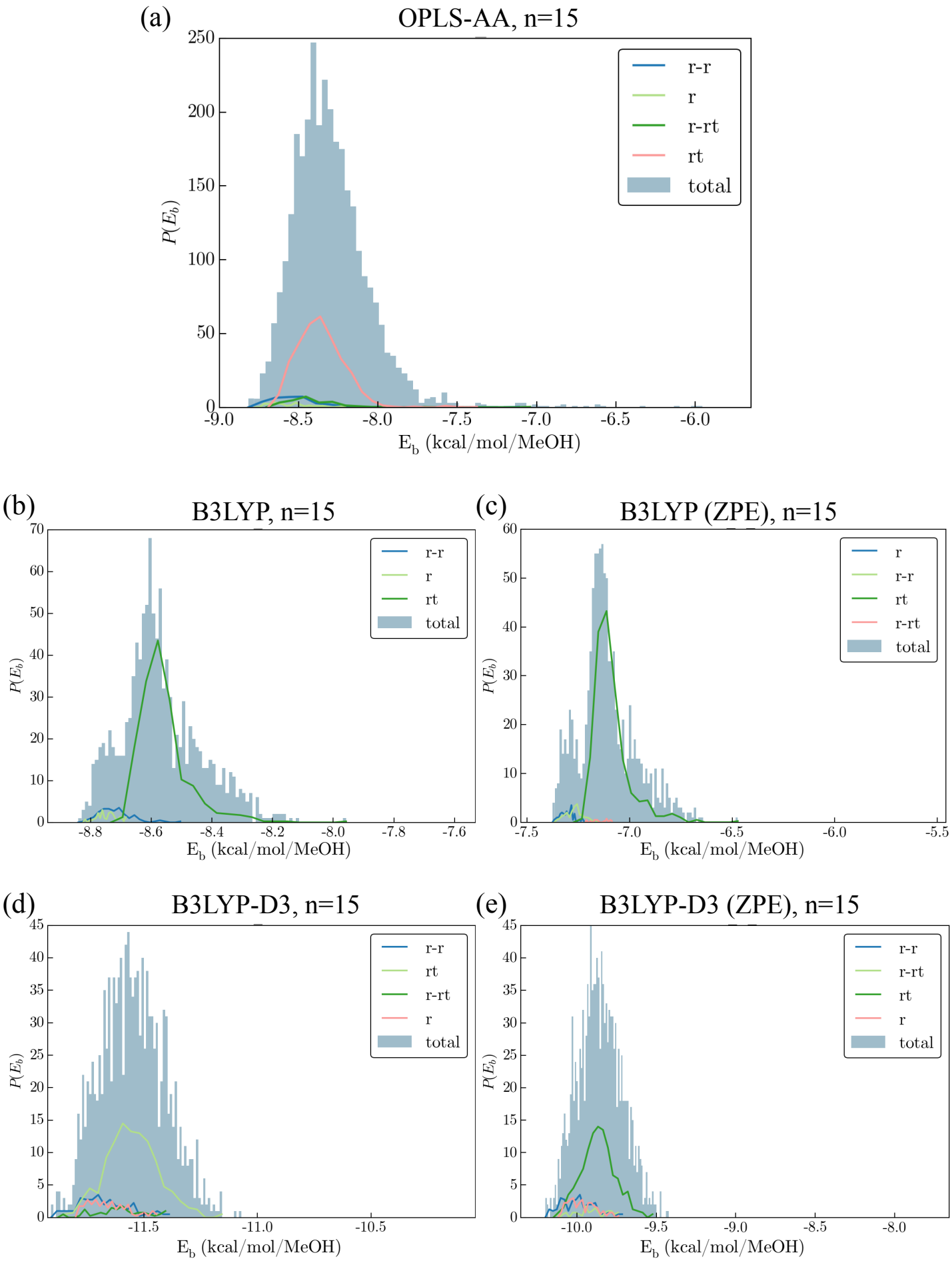

Figure 16s: Energy histograms of $(MeOH)_{15}$ isomers under (a) OPLS-AA, (b) B3LYP, (c) B3LYP with zero-point correction, (d) B3LYP-D3, and (e) B3LYP-D3 with zero-point correction.

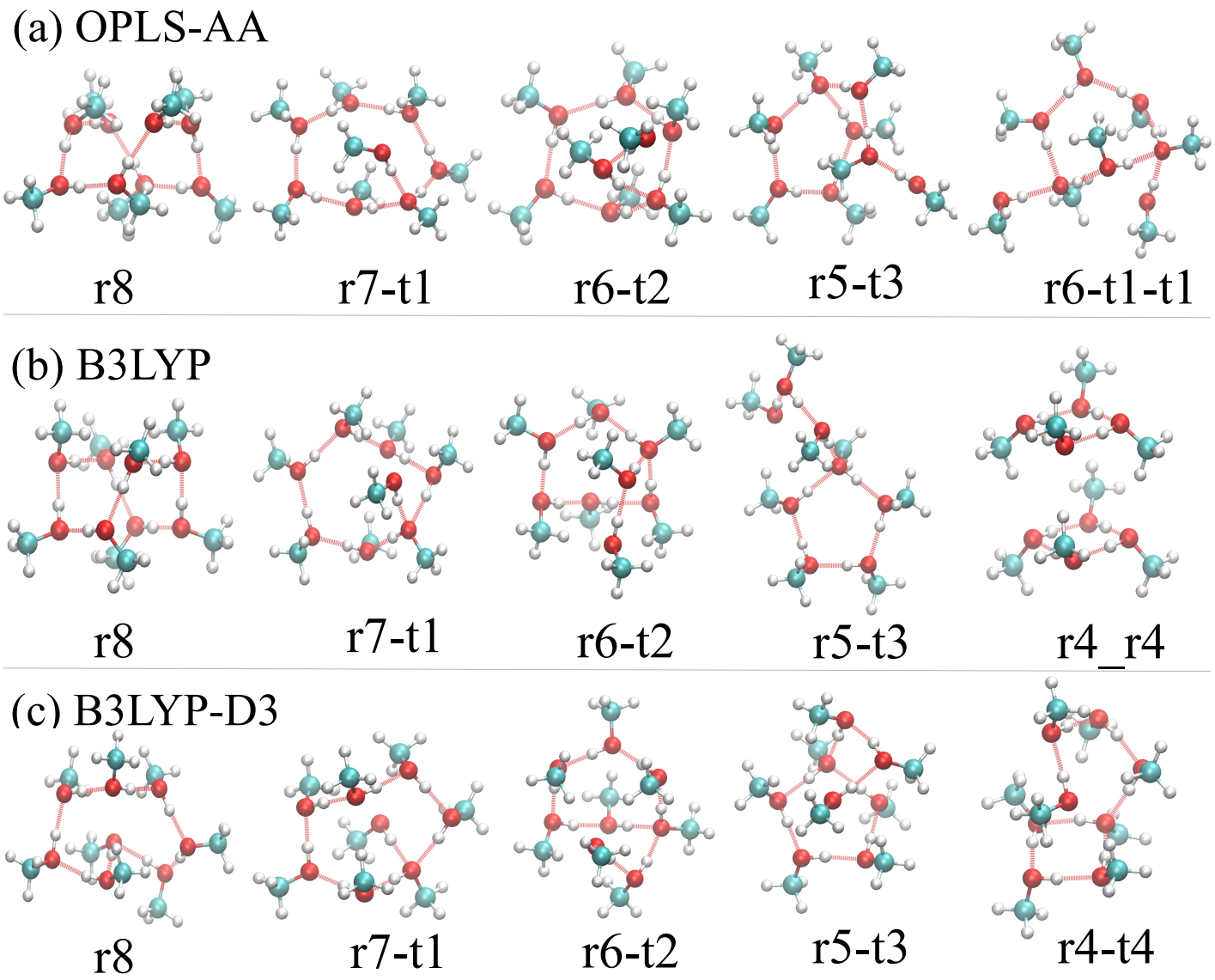

Figure 17s: Structure of the most stable isomers of $(MeOH)_8$ in the leading five topologies of (a) OPLS-AA, (b) B3LYP, and (c) B3LYP-D3 models.

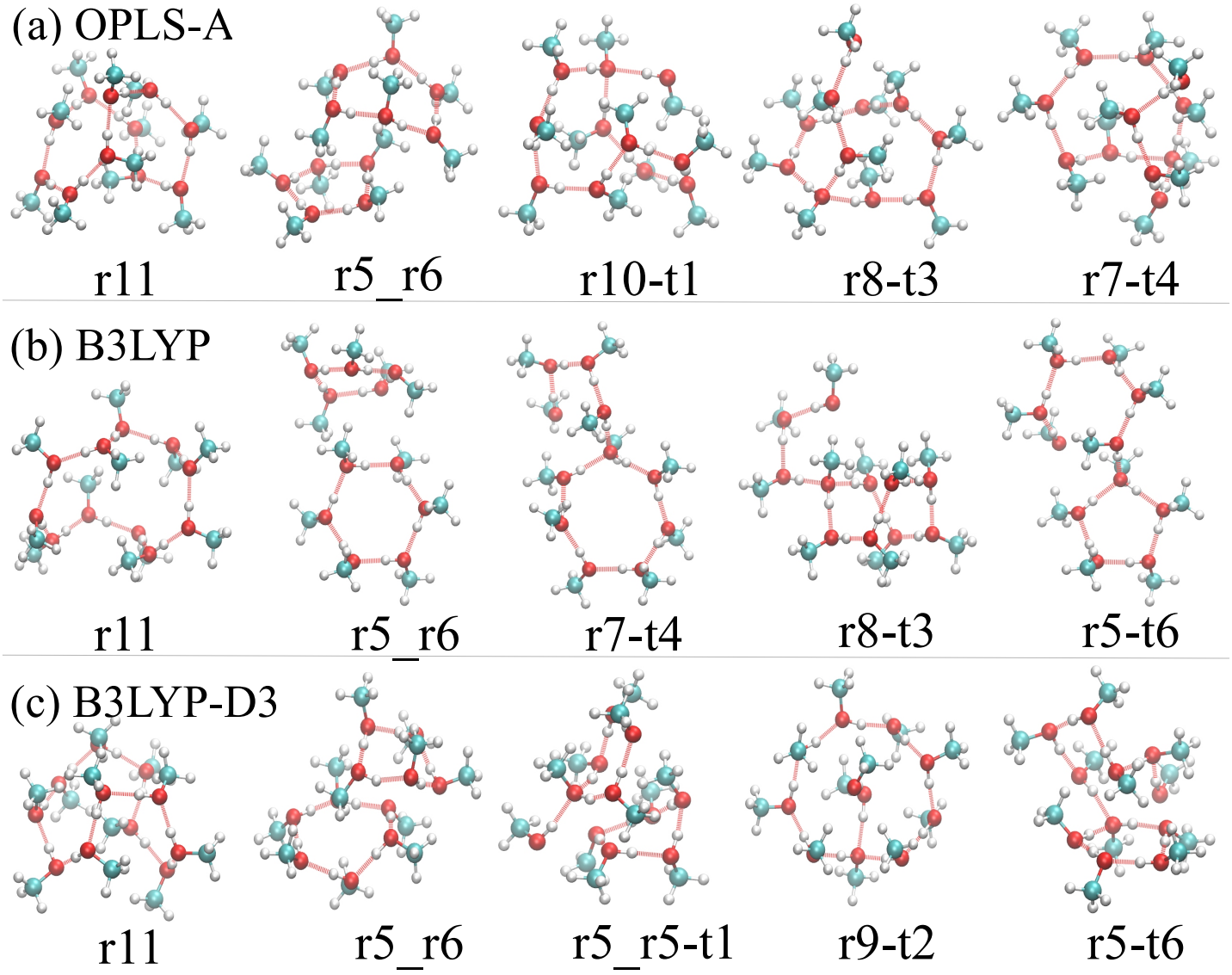

Figure 18s: Structure of the most stable isomers of $(MeOH)_{11}$ in the leading five topologies of (a) OPLS-AA, (b) B3LYP, and (c) B3LYP-D3 models.